FINITE-ELEMENT BASED PRELIMINARYDESIGN PROCEDURES FOR WING STRUCTURES

ICAS-94-9.6.2

F. van Dalen, C. Bil, A. Rothwell
Faculty of Aerospace Engineering
Delft University of Technology
Delft, The Netherlands

P. Arendsen
National Aerospace Laboratory (NLR)
Amsterdam, The Netherlands

Abstract

Two finite-element based design procedures for the preliminary design of wing structures are evaluated and compared with an analytical-empirical wing weight prediction method, as well as with data for the Fokker 100 wing. The quick generation of the simplified finite element model is discussed. The same model is used for both aerodynamic and structural analysis. Allowable stress levels are deduced on the basis of simplified fatigue, residual strength and buckling criteria for standardised structural components. Calculated and allowable stresses, together with nodal displacement limitations, are used in a fully-stressed design process to generate a feasible structural design. An optimum design is also achieved (at greater computing cost, however) using the B2OPT optimization code. Both methods are compared in a study of the effect of aspect ratio on the weight of the Fokker 100 wing.

Notation

$\bar{a}$	dimensionless critical crack length
b	stringer/stiffener pitch
C	design variable linking matrix
c	scaling index for constraints
E	Young's modulus
f	quadratic approximation function for constraints
G	cumulative constraint
g	constraint in main optimization (suffix o denotes before scaling)
g_n	intermediate constraint, i.e. after scaling
g_s	constraint in sub-optimization
K_c	critical stress intensity factor
K_g	stress concentration factor
k	diagonal tension factor
L	rib pitch
n	aircraft load factor
R	radius of curvature of skin panel
R_{gr}	ratio of stress on the ground to stress in 1-g flight
r	constant in cumulative constraint function
t	skin/web thickness
$\hat{t}$	equivalent thickness of stringers/stiffeners
$\bar{t}$	total equivalent thickness ($= t+\hat{t}$)
t_s	stiffener thickness (attached flange)
x,y	design variables (suffix o denotes before scaling)
x_n,y_n	intermediate variables, i.e. after scaling
β	post-buckling ratio
η	compression panel efficiency
η_r	post-buckled 'efficiency' of skin
λ	factor applied to the local buckling coefficient to allow for curvature of the skin
σ	property defined in constraint
σ_{all}	allowable value of property in constraint
σ_{fc}	stress in web stiffener at which forced crippling occurs
σ_L	local buckling stress
σ_N	stress in skin for specified fatigue life
σ_R	stress in the skin at which unstable crack growth occurs in the 'two-bay crack' condition
σ_S	stress in the skin at which stringer failure occurs in the 'two-bay crack' condition
σ_{ult}	average stress in the panel at ultimate load
σ_2	0.2 % proof stress

1. Introduction

Optimization procedures appropriate to the design of a wing structure at the preliminary design stage are developed. The results of optimization at two levels of complexity are compared with a recently developed wing weight prediction method [1]. Particular attention is given to the definition of an optimization model suitable for preliminary design. Some severe simplifications are introduced to enable alternative designs to be explored cheaply and efficiently, nevertheless retaining the essential features of the design. This approach is adopted so that basic aspects of structural design can be included in the overall design concept at an early stage, also with a wider range of loading cases and design conditions.

The optimization procedure is based on a relatively coarse finite-element model of the structure, generated semi-automatically [2]. The same mesh is found to be usable for computation of the aerodynamic loading on the wing. This procedure yields the load distribution throughout the primary structure of the wing, as well as its deformation. If desired the air load distribution can be based on the deformed shape of the wing. Simplification of the optimization model significantly reduces the number of degrees of freedom in the FE analysis. Verification of the structural modelling is, therefore, an essential aspect of the work.

The FE model is not adequate for the detail design of the structure, and in any case the detail design is not of interest to the designer at the preliminary design stage. Defaults are used for standardised stringer shapes, and so on. A number of "standard components" are defined, such as skin panels, spar webs and ribs. For each of these, special purpose optimization routines are developed. Design stresses are deduced in terms of the local loading intensity, load spectrum and fatigue life. Damage tolerance requirements are based on the usual two-bay crack situation. The effect of design limitations such as minimum stringer pitch or thickness limitations due to stiffness constraints are included.

Design of the wing structure is based either on an iterative re-sizing routine, or on a formal optimization using a sensitivity analysis. The first of these rapidly generates a feasible design but is no guaranteed optimum; the second is a much heavier computing task. The results of the two methods are compared to establish to what extent the extra computational effort is justified at the preliminary design stage, also to compare the effectiveness of optimization at the detail design level and at the level of the structure as a whole.

To validate the results obtained, comparisons are made with the weight prediction method referred to above, when the aspect ratio is varied. The design program is being used in a design study of civil transport aircraft in the 300-800 seat categories, in which the effect of aircraft size on the wing weight fraction is investigated.

2. Analysis

2.1 Finite-element model generation procedure.

The creation of a FE-model can be a laborious task even for a small structural component. In conceptual design it would be impractical to redesign the structure in such detail for each different concept; the aim of this work is to implement new ADAS-tools [3] that can be used to assess the effect of alternatives in structural design concepts on aircraft weight and performance at a relatively early stage in the design process. Therefore a proper balance has to be established between, on the one hand, the type and amount of information available and, on the other hand, the suitability of an inherently coarse FE-model to predict stresses, displacements and structural weight with acceptable accuracy.

2.1.1 Definition of skin panels.

The ADAS-system accepts geometry input in the form of a 3-view configuration drawing created with AutoCAD or any other CAD-program that supports the DXF-standard [4]. By means of a protocol that correlates layer names with drawing entities such as lines, text, etc., specific geometric information for the aircraft can be derived and used in the subsequent analysis. Implementing the structural design capability in ADAS required the extension of the ADAS/DXF-protocol to include, for example, the definition of skin panels for the lifting surfaces and the fuselage.

A skin panel in a lifting surface is defined by drawing the four edges of a quadrangle in the planform outline, as shown in figure 2.1. For the fuselage a

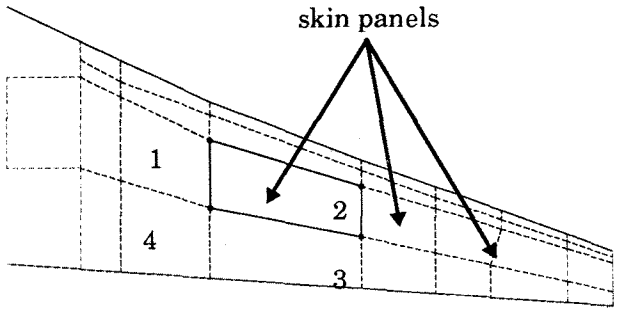

Figure 2.1: ADAS representation of the structural layout of the Fokker-100 wing.

similar procedure is followed. Through the layer name definition each skin panel is uniquely identified.

2.1.2 Finite-element model generation program.

The 3-view drawing with skin panels can subsequently be transformed into a FE-model by a mesh generation program. It proved impractical to develop a single mesh generation program that automatically creates a FE-model for all possible types

of structural configuration. Instead, it was found that a toolbox approach would be more suitable; the designer creates a mesh generation program tailored to the type of aircraft being studied, but to facilitate the development of such a program the ADAS system provides an number of subprograms that can be used as building blocks. Although this approach requires some programming skill on the part of the designer, the flexibility of system is greatly improved.

Association of the three orthogonal views in the configuration drawing defines a schematic geometric model, which forms the basis of the FE-model constructed from mesh areas. A mesh area N is a 3-dimensional surface enclosed by 4 spatial curves and represented by a regular grid of NI(N) times NJ(N) node points in two directions, as shown in figure 2.2. To create a mesh area, the

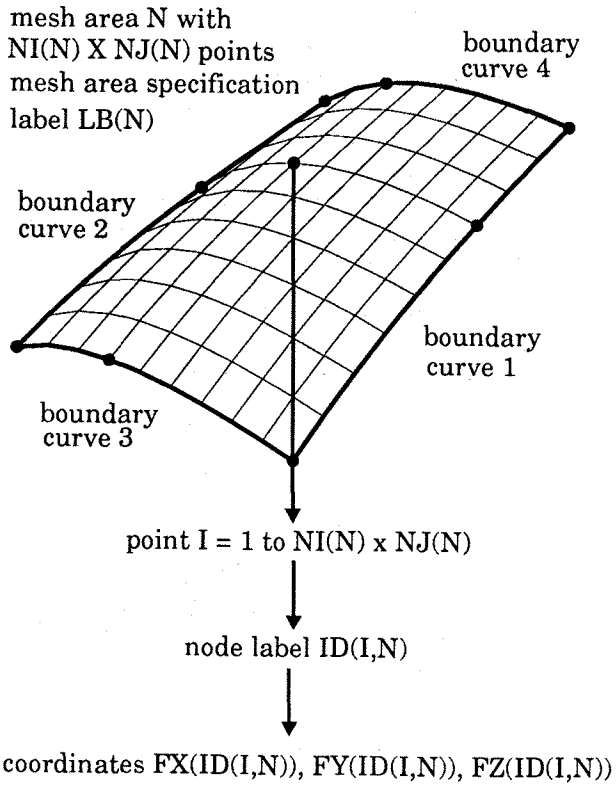

Figure 2.2: Definition of a mesh area.

nodes on the four boundary curves must first be determined from the panel definition and the geometric model. The second step is then to generate the internal nodes by interpolation between the boundary nodes. This procedure is repeated for all skin panels in the structure. The ADAS program library contains basic subprograms that can readily be used to facilitate the development of a specific mesh generation program. For example, the subprogram DXLMSH (X1,Y1,X2,Y2,I1,I2,IP,KS,LS,K) calculates the X- and Y-coordinates of node I1 to I2 for a specified number of equidistant nodes IP along the projected line (X1,Y1) to (X2,Y2). The corresponding Z-coordinate is calculated by interpolation assuming a ruled surface between pairs of airfoil sections. The parameter LS is the lifting surface reference number and KS denotes the upper or lower skin (KS = 1 and KS = 2 respectively). DXLMSH will also assign new node labels by incrementing a node counter. This process is repeated for the four edges of the mesh area K = 1,2,3,4. The subprogram DCROS (LB,N) can subsequently calculate the coordinates of the internal nodes by interpolating between the edge nodes using Coons method. DXCROS associates a user-defined label LB with the mesh area signifying the type of structure, the type of elements used and the material. The significance of the LB-parameter is discussed in more detail in section 2.3. DXCROS increments a mesh area counter N which can be used at a later stage to refer to the mesh area or to the nodes therein, e.g. to link another mesh area to it.

The subprogram DXLINK can be used to establish a logical connection between a new mesh area and an existing one by using the nodes on the common edge as boundary points. Only the node labels are copied, not the coordinates. The rest of the procedure goes as described above. Because the common edge nodes have the same node labels they will point to the same coordinates. This ensures the consistency of the topology.

Beam/rod elements are treated as a mesh area with one row of nodes (NJ(N) = 1), so only one edge (K = 1) needs to be defined. DXCROS will automatically skip the creation of internal nodes and will simply create a new mesh area reference number N.

The previous section was mainly concerned with the procedure to generate a physical FE-model. Such a model will usually be rather coarse and highly simplified. It contains only shell/membrane and beam/rod elements and the number of nodes is kept small to reduce CPU-time. However, to improve the representation of the model the designer can specify additional information through a user-defined specification label LB associated with each mesh area by the subprogram DXCROS. This parameter is a multi-digit code which signifies the aircraft component that the mesh area is part of, the type of structure and the material.

Although the coding, debugging and testing of a mesh generation program for a complete aircraft structure may require some effort, the actual time to compute the FE-model is only about 5 seconds

for a model of around 1000 elements. Because the data structure is well defined and has a consistent topology, modifications to the mesh generation program are relatively easy to implement. So long as the topology is not altered, changes to the configuration drawing will not require modification of the mesh generation program.

2.1.3 Model rendering and data display.

It is good practice to check the FE-model visually at regular intervals during the development of a mesh-generation program. For this purpose a set of AutoCAD-interface modules have been developed to show the FE-model and to display analysis results, as illustrated in figure 2.3. A FE-model

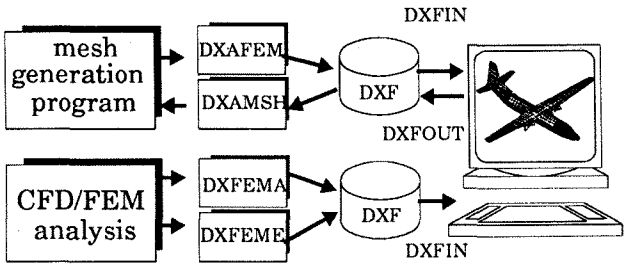

Figure 2.3: ADAS tools for the display of an FE-model and analysis results in AutoCAD

can be displayed in AutoCAD with individual mesh areas drawn as single entities. Each mesh area will be associated with a layer name of the form SHELL_N_LB (shell elements) or BEAM_N_-LB (beam elements), where N and LB denote the mesh area number and the specification label as described in the previous section. Shell elements or beam elements can be displayed separately by switching off the appropriate layers. This is illustrated in figure 2.4 for the Fokker-100 wing struc-

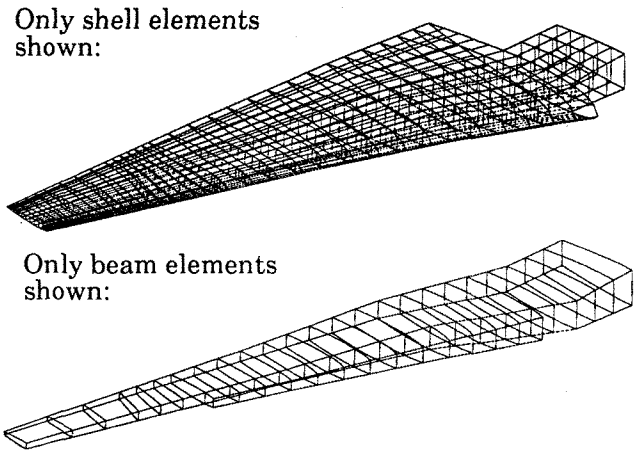

Figure 2.4: Finite-element model representation of the Fokker-100 wing structure.

ture already seen in figure 2.1.

Nodes and their associated node labels can also be plotted in the FE-model. Coincident nodes are automatically detected and plotted in red. Transferring an FE-model between ADAS and AutoCAD is a two-way process, i.e. a structure drawn or modified with AutoCAD can also be transferred back into the ADAS internal FE-data structure. This facility can be used to make small modifications to the FE-model, e.g. to make cut-outs and to define attachment points. When a FE-model is imported from a DXF-file, each mesh area N defined in the data structure is overwritten by the imported mesh area with the corresponding reference number. Mesh areas with a unique reference number will simply be added. A check is made to see if the imported structure has nodes coincident with the model already in the data structure and, if so, a logical link will be established.

Other subprograms are available to superimpose analysis results on to the FE-model. The analysis results may be vector (velocity, force, etc.) or scalar (pressure distribution, stress levels, etc.). To display analysis results, the mesh areas in the FE-model are broken down into separate facets. Vector data is plotted as 3-dimensional arrows with scaled length, while scalar data is represented by a color code for each facet.

2.2 Aerodynamic analysis

For the subsequent structural analysis it is necessary to determine the most critical load cases and to calculate the resulting loads on each element of the FE-model. To estimate aerodynamic forces under a given flight condition an existing panel code O215 was adopted [5]. The O215-program is based on linearized potential flow theory and was originally developed by the National Aerospace Laboratory (NLR). The method is particularly suitable for the prediction of pressure distributions around smooth objects in subsonic flow. As with a FE-model, an aerodynamic panel model requires a wetted surface representation by separate panels. It would be convenient if one model could be used for both aerodynamic and structural analysis. However, a panel distribution that is optimal for aerodynamic calculations is generally different to that for FE calculations.

A study was made to investigate the effect of the distribution and orientation of panels on the calculated pressure coefficients [6]. It was shown that for the purpose of predicting aerodynamic loads the effect is negligible. This implies a significant

simplification and a reduction in turn-around time of results by using the *same* mesh for both structural and aerodynamic calculations, as illustrated in figure 3.5. The O215-program, in particular the

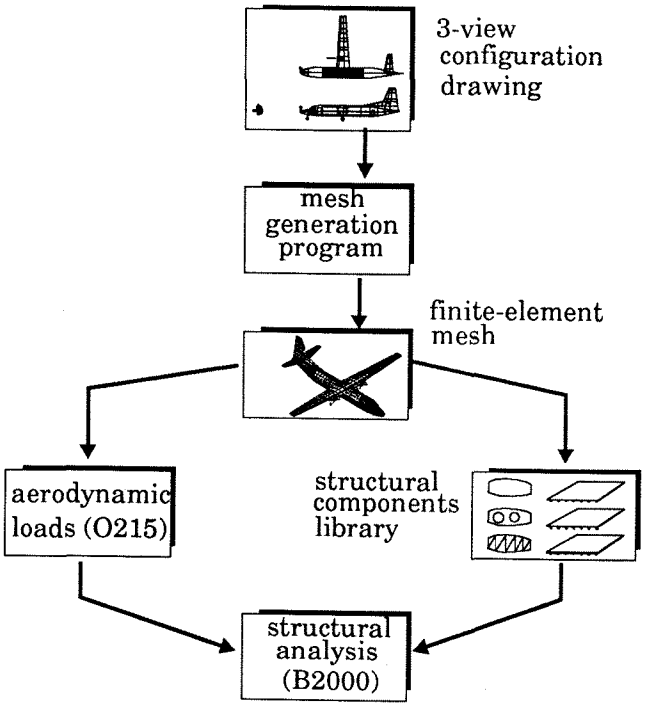

Figure 2.5: Integration of aerodynamic load prediction and structural analys based on one model.

input processor, had to be modified to match the FE-model data structure to the ordering of panels required by O215. This is done on the basis of specification labels defined for each mesh area. For example, if LB < 0 then the corresponding mesh area is part of an internal structure and is automatically removed from the aerodynamic model. Other definitions allow O215 to distinguish between lifting and non-lifting bodies.

2.3 Structural analysis

To perform a finite element analysis, the elastic properties of the model and the mass distribution must be defined. The mesh areas generated as already described are represented in the F.E. model according to their structure class and material. The structural data base supports the following classes of wing structural components:

(I) stringer-skin panels

(II) stiffened spar webs

(III) ribs

(IV) end load carrying members

The stringer-skin panels (featuring either Z, hat or blade stringers) are modelled as composite membrane elements with one layer of isotropic material to represent the skin, and one layer of orthotropic material (with uni-directional stiffness only) to represent the stringers. For the stiffened spar webs, only the webs are represented in the FE model. The elastic constants of the web material are modified to achieve a spar bending stiffness conforming to Engineer's Bending Theory. The spar web stiffeners are used only in the calculation of the allowable shear stress in the spar web (see section 3.2). Two types of rib structure are supported: a plate rib, represented as a Z-section stringer-skin panel, and a truss rib. The latter is represented as an element with a single layer, with a shear stiffness equivalent to that of the standardised truss rib. End load carrying members are represented as rod elements with axial stiffness only.

All structural components are thus modelled using either membrane or rod elements having only three degrees of freedom per node. The skin panels do not therefore have the bending stiffness required to carry aerodynamic loads. Linear displacement constraints are used to relate the displacements of free nodes in the skin to the deformation of the adjacent ribs. This results in a load transfer from the skin into the ribs, much the same as would result if individual stringers with bending stiffness were used. Due to the smaller number of degrees of freedom, however, FE processing times and required disk space are drastically reduced.

As well as aerodynamic loads, inertia loads acting on the various mass contributions to the wing are an essential aspect of the wing loading. The total wing weight is broken down into a primary structure weight and a secondary structure weight (high lift devices, ailerons and fixed leading and trailing edges). The primary structure weight, as represented by the mass of the finite element model, does not include the weight increases caused by reinforcements around cut-outs and panel joints, and the presence of the landing gear mountings etc. These weight contributions, as well as those of the secondary structure, are estimated using Torenbeek's method [1] and added to the nodes of the FE model in an appropriate way. An inertia force corresponding to the acceleration in each loading condition is then applied to each node of the model. With all the loads applied, the model is supported at the wing-fuselage connection points, and a finite element analysis performed.

Figure 2.6 shows the deformation of the structure under a typical up-gust loading condition.

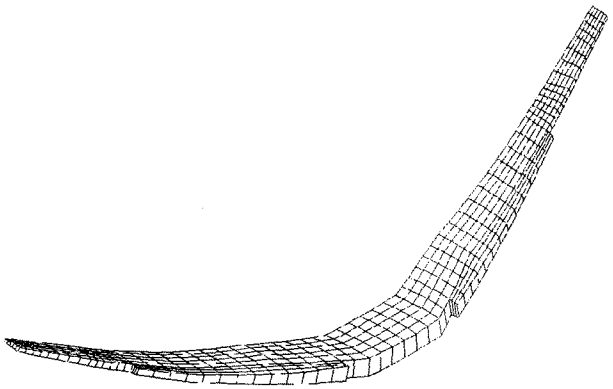

Figure 2.6: Deformation of the wing structure

3. Constraints

Certain constraints are introduced immediately into the structural optimization. These include stiffness constraints, defined by the maximum displacement at specified points in the structure in a particular loading condition, and lower bounds on skin thickness and on the equivalent thickness of stiffeners of various types. Stiffness constraints can refer to the torsional and flexural stiffness of the wing, and to local deformation of the skin affecting the aerodynamic profile. Certain other constraints, in particular flutter constraints, depend on the stiffness and mass distribution over the structure as a whole. Implementation of these is not yet complete, and no further discussion will be made here. Static aeroelastic effects - divergence, aileron reversal - can be treated in an iterative manner by analysis of the deformed structure, should this be necessary. The remaining constraints, of particular concern in this section, are stress constraints on the design of the structure. For this purpose the four classes of structural component already identified are:

(I) stiffened panels (i.e. wing skins) in tension or compression combined with shear load;
(II) shear webs (i.e. spar webs and 'heavy' ribs), which may be either transversely stiffened or unstiffened plate webs;
(III) 'standard' wing ribs, either stiffened plate webs or alternatively truss ribs;
(IV) end load carrying members (e.g. spar flanges and local reinforcement).

The object of the design procedures developed for these components is to obtain reasonable estimates of the allowable stresses in an efficiently designed structure, to enable an initial sizing to take place. It is of course essential that these allowable stresses respond in the right way to changes in design - local loading intensities, rib pitch, minimum thickness, etc. - and at the same time that the stress levels used can actually be realised in later stages of detail design. The allowable stresses are based on the following considerations:

- material allowable stresses
- buckling and post-buckling behaviour
- specified fatigue life
- residual strength requirement, i.e. cracked structure

Table 3.1 defines the specific constraints applying to each class of component. All constraints are eventually reduced to an allowable stress level, e.g. fatigue is expressed not as an expected life of the structure but as an allowable stress level to achieve the required fatigue life; failure of the stiffeners of a post-buckled shear web is expressed not as a stress in the stiffeners but as a corresponding shear stress in the web.

Constraint (1)	I Wing skins	II Sparwebs (2)	III Wing ribs (3)	IV E.L.C. memb. (4)
Minimum thickness	x	x	x	x
Min. stringer/ stiffener pitch	x	x	x	
Material yielding	x	x	x	x
Material fracture	x	x		x
Initial buckling	x	x	x	
Post-buckling	x	x		
Fatigue life	x			x
Residual strength	x			

Table 3.1: Constraints applying to each class of structural component

(1) Displacement constraints (e.g. torsional stiffness) not included because these relate to the FE model rather than to individual structural components.
(2) Also 'heavy' ribs.
(3) Min. pitch constraint does not apply to truss ribs.
(4) Spar flanges and local reinforcement.

It will be appreciated that no comprehensive detail design can be carried out at this stage of optimization of the wing structure. Since the calculation of allowable stresses is performed very many times during the whole optimization process and for all components of the structure, rather simple analysis methods are preferred. This implies use of standard engineering formulae rather than more sophisticated methods. These will be discussed further in the following paragraphs, in relation to each class of structural component in turn. Although limitations must be placed on the design of components, the design follows as closely as possible the usual design practice. For example, stringer-skin panels are allowed Z-section, hat-section or integral (blade) stringers, but these have fixed ratios of stringer height to thickness, etc. This greatly reduces the number of design variables.

3.1 Wing skins

Wing skins (class I) are stiffened panels under combined tension/compression and shear. They are distinguished from shear webs by having stringers in the longitudinal rather than the transverse direction. In compression, local and flexural buckling modes are considered. Local buckling coefficients for panels with the three types of stringer are stored as data and interpolated in the computer. A reduction factor is applied to the local buckling coefficient to allow for shear load on the panel, based on the well-known parabolic interaction formula. A further factor

$$\lambda = 1 + \frac{1}{400}\left(\frac{b^2}{Rt}\right)^2$$

is applied to the local buckling coefficient to allow for curvature of the skin. In fact this is a highly simplified approach which aims to find a lower bound to the average/edge stress curve, thereby avoiding the unstable, highly imperfection sensitive buckling and post-buckling behaviour of a curved plate. The minimum load at which local buckling may occur, defined by

$$\sigma_L = \frac{\sigma_{ult}}{\beta},$$

must be specified. For post-buckled panels the 'tangent area' of the skin $\eta_r bt$ is used in Euler's formula for flexural buckling. An appropriate expression for η_r, in agreement with the formula for λ above, is

$$\eta_r = 0.4\left[1 - 0.0006\left(\frac{b^2}{Rt}\right)^2\right]$$

The Ramberg-Osgood formula is used for the tangent modulus (for local and flexural buckling). The compressive stress (in the *stringer* for a post-buckled panel) is limited to the 0.2 % proof stress. Local buckling of the stringer itself is avoided by use of a relatively sturdy stringer.

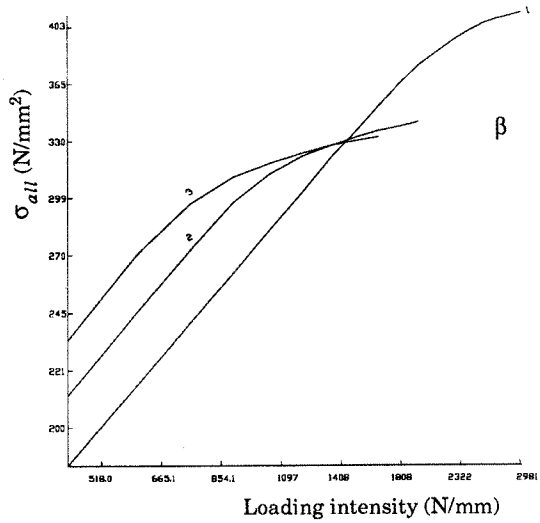

Fig. 3.1: Optimized compression panel

Figure 3.1 plots the maximum allowable stress for a flat, aluminium alloy, Z-section stringer-skin panel as function of loading intensity, by the procedure given above. The unbuckled panel ($\beta = 1$) shows the characteristic behaviour, with an acceptable efficiency [7] $\eta = 0.75$. At low loading intensity the post-buckled panel ($\beta = 2$, $\beta = 3$) shows the expected moderate improvement over an unbuckled panel. Stringer pitch and ratio t/i are varied in fig. 3.1 for an optimum panel (i.e. within the limitation imposed by a standard shape of stringer).

In tension the allowable stress is based on the fatigue life and on the residual strength of the cracked structure. Fatigue life is based on a Miner's law calculation. A loading spectrum is derived from cumulative frequency curves for air and ground loads given in [8] and [9]. A number of loading cases must be analysed to obtain an average stress in each panel, and a stress level corresponding to a reference load. A stress concentration factor is used appropriate to the type of panel ($K_g = 4.5$ for riveted stringers). An iterative procedure deduces the allowable stress level σ_N to achieve the specified fatigue life. Figure 3.2 plots the allowable 1-g stress level for a particular loading spectrum as function of the aircraft load factor n in a 10 fps reference gust (R_{gr} is the ratio of the average stress on the ground to the stress in 1-g flight). The allowable fatigue stress responds therefore to

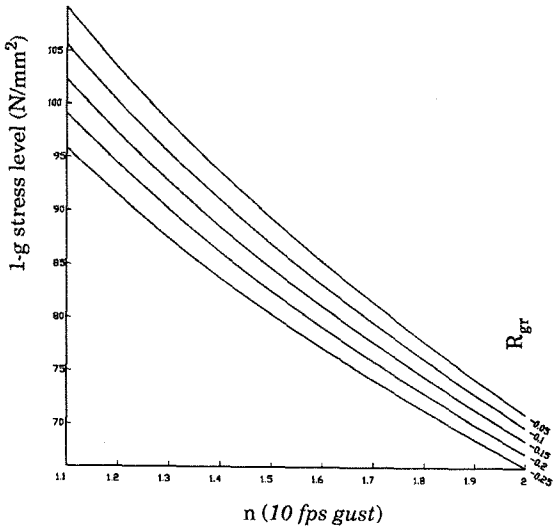

Fig. 3.2: 1-g fatigue stress level

aircraft parameters such as wing loading and aspect ratio, as well as relating directly to the mission profile and required life.

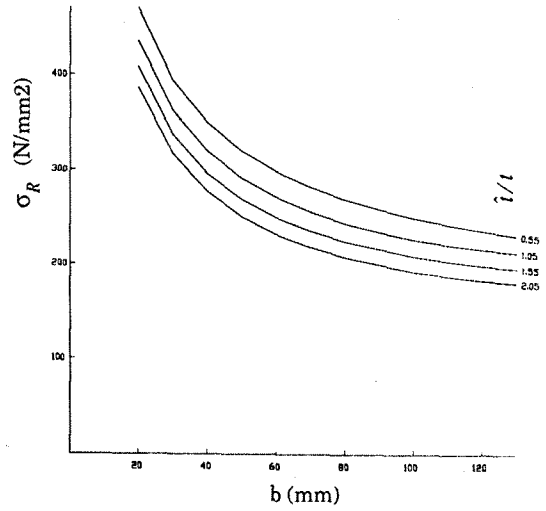

Fig. 3.3: Residual strength of the skin

Residual strength is based on the 'two-bay crack', i.e. a broken stringer and a skin crack running to the adjacent stringer on each side. Figure 3.3 shows a typical plot of residual strength against stringer pitch, for various $\hat{t}/t$ values, from which the following empirical formula is deduced for the stress in the skin at which unstable crack growth occurs in this condition:

$$\sigma_R = \sigma_2 \left[1 - 0.152\frac{\hat{t}}{t}\right] \left[0.143\bar{a} + 1.056\right] \frac{1}{\sqrt{\bar{a}}}$$

$$\bar{a} = 1.1b\frac{\pi}{(K_c/\sigma_2)^2}$$

where K_c is the critical stress intensity factor for the skin material, σ_2 is the material yield stress and $\bar{a}$ is the dimensionless critical crack length (the critical cracklength is assumed to be 10 per cent greater than the stringer pitch). The stress σ_R may be regarded as an allowable stress for residual strength. Due to the presence of the crack, additional stress is induced in the stringers. A corresponding formula is developed for the stress in the skin at which failure of the stringers occurs under the same damage condition:

$$\sigma_s = 1.09\sigma_2 \left[1.57 - (\bar{a} + 10.1)\,(0.0518 + 0.0143\frac{t}{\hat{t}})\right]$$

The stresses σ_N, σ_R and σ_S for fatigue and residual strength are included, together with the usual material allowables and the allowable stresses for buckling, in both levels of the structural optimization.

3.2 Spar webs, ribs and end load carrying members

Shear webs (class II) are flat panels, either unstiffened or with double-sided, angle-section stiffeners placed transversely on the web, loaded only in shear. Buckling coefficients obtained from [10] are stored as data and interpolated in the computer. The buckling stress depends on the flexural stiffness of the web stiffeners (if present) and therefore the design takes into account the possibility that stiffeners of reduced stiffness may be more efficient at small stiffener pitch. The secant modulus is used to correct for yielding. If a post-buckling design is permitted, the user must specify the post-buckling ratio β (limited to $\beta \leq 5$). The design requirements are then the maximum stress in the buckled web (ultimate load), the onset of yielding in the web (limit load), and forced crippling of the stiffeners. In a well designed web at moderate values of β, column failure of the stiffeners is highly improbable, also additional stresses in the spar flanges are relatively small. Data for the stresses in the web and stiffeners are taken from [11]. For forced crippling of the stiffeners the following formula is used:

$$\frac{\sigma_{fc}}{\sigma_2} = 0.5k^{2/3}\left(\frac{t_s}{t}\right)^{1/3}$$

where k is the diagonal tension factor, t is the web thickness and t_s the thickness of the stiffener (i.e. attached flange).

So-called 'heavy' wing ribs (i.e. those that support

major load inputs such as at flap attachments) are represented as shear webs with discrete end load carrying members for rib flanges and other concentrated members where indicated. A different approach is adopted for 'standard' ribs (class III), which are much lighter in construction and for which local loads, such as crushing loads, are more significant. These may be either plate ribs or truss ribs. Plate ribs have transverse, Z-section stiffeners on one side only, and are treated as compression panels under the action of crushing loads together with shear stress in the rib. Truss ribs have 60° bracings and chordwise members running inside the stringers of the wing skins. Standard channel-sections, i.e. with fixed dimensional ratios, are adopted for both the bracings and the chordwise members. For truss ribs the strength requirements refer to flexural buckling of the bracing members, and to the bending stress in the chordwise members. These carry local loads between the supporting points of the bracings. An equivalent 'web thickness' t of a truss rib is deduced on the basis of effective shear stiffness; the equivalent stiffener thickness $\hat{t}$ is deduced so that $(t+\hat{t})$ represents the mass of the rib.

Finally, the design of concentrated end load carrying members (class IV, i.e. 'heavy' rib flanges, but also spar flanges and other reinforcement) requires little further comment. It is assumed that these are compact members for which buckling plays no role. Their allowable stress is, therefore, either the material allowable stress or a fatigue stress limit based on an appropriate stress concentration factor.

4. Optimization

Optimization of the structural model is performed at two levels. At the main optimization level, material is distributed between the various structural components. Design variables at this level are the equivalent (i.e. smeared) thicknesses t of the skin and stringers or stiffeners. For a rib an effective t is defined above; for an end load carrying member only the cross-sectional area is a design variable. At the sub-optimization level, material is distributed within the structural components. In the case of a stringer-skin panel or a stiffened shear web, the sub-level design variables are the ratio $\hat{t}/t$ of the equivalent thickness of the stringers or stiffeners to the skin thickness, and the stringer or stiffener pitch. There is no sub-optimization of truss ribs.

4.1 Main optimization

The structural model is optimized using B2OPT [12], a module developed within the finite element program B2000 [13]. B2OPT is capable of analyzing and optimizing a general finite element model. Its design variable types include: shape variables, material properties, forces, nodal masses, and sizing variables. Constraint types within B2OPT are: displacement, strain, stress, reaction force, frequency, eigen mode, mass, linear buckling and all kinds of gauge limits. In this study, only a limited set of B2OPT capabilities is used. All the variables used represent actual or equivalent thicknesses and cross-sectional areas, while only stress and displacement constraints are used.

B2OPT is organised in a modular fashion using the data base management program MEMCOM [14] to communicate between its major sub-modules. The B2OPT flow chart, figure 4.1, shows a loop (or maxi-cycle) of sub-modules. The organization of B2OPT is based on the "approximate model" concept. With this concept it is possible to seperate the main three computational blocks of the optimization process as follows:

- exact function evaluation, based on FEM calculations and "Analysis Model" data. These computations are performed by the sub-modules B2SR and B2CO.
- exact function gradient evaluation, based on sensitivity analyses. These computations are performed by the sub-modules B2GSR and B2GCO.
- design optimization, based on approximations of the constraints and objective. These computations are performed by the sub-modules B2CAM, B2OAM and B2RAM. This optimization is often referred to as "approximate model optimization".

One maxi-cycle of the optimization consists of the sequence: exact function evaluation, exact function gradient evaluation and "approximate model optimization". These maxicycles are repeated until an optimum of the exact problem has been reached.

The "approximate model" concept implies that quadratic approximations of all CPU expensive constraints (f) in terms of the design variables (x) are used during the actual optimization:

$$f \cong f_0 + f'x + \frac{1}{2}f''x^2$$

Since only the approximated functions are

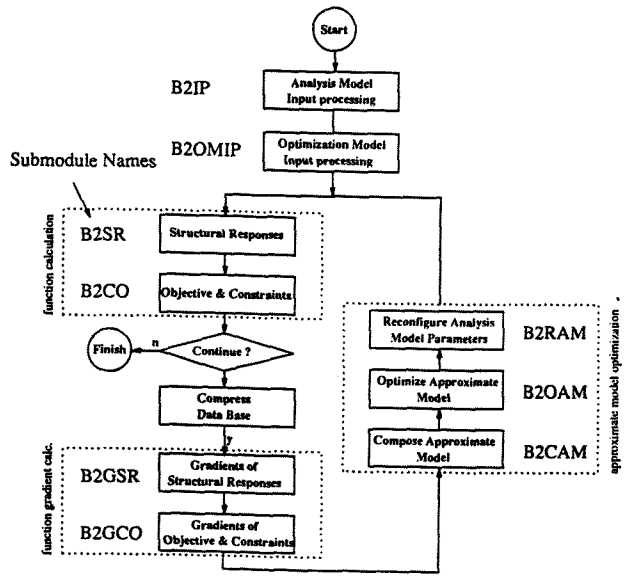

Figure 4.1: B2OPT flow diagram

optimized the loop is repeated until a true optimum is found. The linear part of the approximation is based on gradient calculations, while the quadratic part is based on the Broyden-Fletcher-Goldfarb-Shanno (BFGS) update method. This concept results in a reduction in the number of CPU expensive function evaluations (FEM calculations) and is therefore relatively fast.

Within the optimization, linking is used to reduce the number of independent design variables. Linking implies that the change of "Analysis Model Parameters" (AMP) such as element thickness and nodal coordinates are directly related to the change of design variables (x). This (linear) relation is expressed by the so-called linking matrix C:

$$AMP_{new}{}^{i} - AMP_{old}{}^{i} = C_{ij}(x^{j}_{new} - x^{j}_{old})$$

Normalization of design variables is used to obtain design variables of the same order of magnitude during optimization. Design variable normalization implies that the original design variables are divided by their initial values. Constraints are normalized in the usual manner; a constraint written as: $\sigma \le \sigma_{all}$, when normalised is written as: $\sigma/\sigma_{all} - 1 \le 0$. Notice that σ in these formulae denotes any property to be constrained, for example a displacement or a buckling load. Besides normalization, so-called scaling techniques are used to improve the accuracy of the approximations used in the approximate model concept. These techniques are applied to both design variables and constraints. The "scaling order" technique applied to the design variables is well known in the literature and creates what are often referred to as "intermediate variables":

$$x^{i}_{n} = (x^{i}_{o})^{s^{i}}$$

The same principle is also applied to constraints, resulting in "intermediate constraints" (see ref. [12] and [15]). Constraints are usually written as:

$$g^{j}_{o}(x) = \frac{\sigma}{\sigma_{all}} - 1 \le 0$$

Applying the "scaling order" technique to constraints changes the format in which they are written. The constraints can be expressed as follows:

$$g^{j}_{n}(x) = \frac{c^{j}}{|c^{j}|}\left(\left[g^{j}_{o}(x) + 1\right]^{c^{j}} - 1\right) = 0$$

$$= \frac{c^{j}}{|c^{j}|}\left(\left[\frac{\sigma}{\sigma_{all}}\right]^{c^{j}} - 1\right) \le 0$$

The scaling order technique applied to design variables and constraints can be used to transform the design space in such a way that inside this space, the scaled constraints are approximately linear functions of the scaled design variables. This is easily understood by considering the following example. Suppose there are three constraints (g^1, g^2, g^3) as a function of two variables (x,y):

$$g^{1}_{0}(x_0, y_0) = \left[x_0^{-1} + y_0^{3}\right]/\sigma_{all} - 1$$

$$g^{2}_{0}(x_0, y_0) = x_0^{2}/\sigma_{all} - 1$$

$$g^{3}_{0}(x_0, y_0) = \left[x_0^{-2} + y_0^{6}\right]/\sigma_{all} - 1$$

This set of highly non-linear constraints can be transformed using the following "scaling order" constants: $s^1 = -1, s^2 = 1/3$, $c^1 = 1$, $c^2 = -1/2$ and $c^3 = 1/2$:

$$g^{1}_{n}(x_n, y_n) = \left[x_n + y_n\right]/\sigma_{all} - 1$$

$$g^{2}_{n}(x_n, y_n) = x_n\sqrt{\sigma_{all}} - 1$$

$$g^{3}_{n}(x_n, y_n) = \sqrt{\left[(x_n)^2 + (y_n)^2\right]}/\sigma_{all} - 1$$

These transformed constraints have a far better behaviour during optimization, being linear functions. Generally is not possible to choose the scaling order constants in such a way that *all* scaled constraints are linear functions. The non-zero second order behaviour of these scaled constraints will however, be dealt with by the BFSG method as used in the approximate model

concept. The scaling order constants can be calculated using the method described in reference [15].

4.2 Sub-optimization

For the sub-level design variables (the panel thickness ratio $\hat{t}/t$ and the stringer or stiffener pitch) a sub-optimization is performed for each component. In this sub-optimization the degree of constraint violation is minimized by means of a cumulative constraint defined:

$$G = \frac{1}{r} ln \sum_j e^{r g_s}$$

where g_s are the individual constraints ($g_s \leq 0$) and r is an appropriately chosen constant. Apart from the stress constraints discussed in section 3, a shear stiffness constraint is also included in the cumulative constraint definition of each stringer-skin panel or shear web. This local stiffness constraint is based on the torsional stiffness requirement at the main level, and ensures that panels which have critical stiffness at the main level are not reduced in thickness to meet strength requirements in the sub-level. Because the formulae involved in the analysis of components are relatively simple and rapidly evaluated, sub-optimization can be by a zero-order method (based on the Hooke and Jeeves method [16]). This has, besides simplicity, the particular advantage of not being upset by discontinuities such as the loss of stiffness that occurs when passing from an unbuckled to a post-buckled design (a relatively large initial step must be chosen to avoid being trapped in a local optimum that occurs here). The sub-optimization is then unconstrained except, of course, for side constraints such as minimum stringer pitch. Rather less obvious is the need for independence of the design stresses between different components; for example, the buckling stress of a spar web in shear is to some extent dependent on the bending stress in the spar flanges. This is ignored, to avoid coupling between different components.

A special action was found necessary to improve the interaction between the two optimization levels. While in the sub-level the panel thickness ratio $\hat{t}/t$ and the stringer or stiffener pitch b are varied in effect to achieve the highest possible allowable stress levels (see fig. 4.2), these allowable stresses still remain highly sensitive to the total equivalent thickness $\hat{t}$ of the panel. The equivalent thickness $\hat{t}$ is optimized at the higher level for *constant* allowable stress levels, which may result

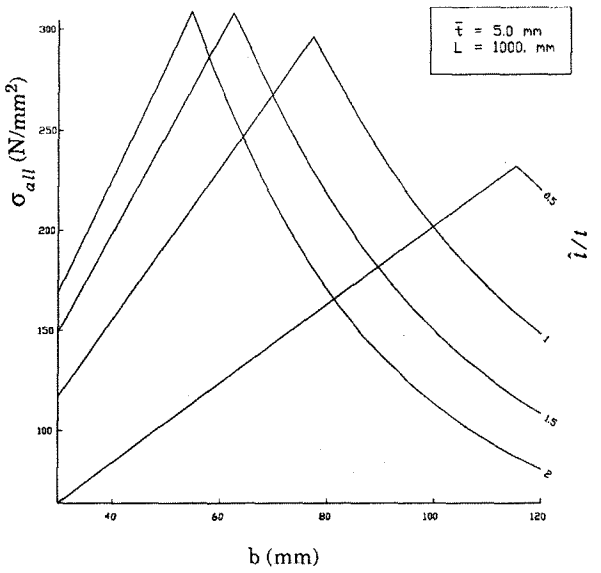

Fig 4.2: Allowable stress as a function of panel thickness ratio and stringer pitch

in divergent oscillations in the thicknesses when moving from one level to another. To prevent this, the equivalent thickness is also allowed to vary in the sub-level optimization. This could be seen as 'taking an advance' on the expected changes in the main optimization, and means that all panel variables are optimized in the sub-level to reach the highest possible stress levels for a loading intensity determined at the main level. After a sub-level optimization, only the allowable stresses and the values of $\hat{t}/t$ are, however, returned to the main level, while the equivalent thicknesses retain their optimum values as found at the main level. In this way, the allowable stresses change only when changes in the stiffness distribution of the structure result in changes in local loading intensity. These changes are generally quite small and therefore allow rapid convergence.

5. Application

For the purpose of this design study, the Fokker 100 wing was selected as a suitable basis for comparison. Due to the moderate aspect ratio of the wing and the fuselage mounted engines, it may be expected that a satisfactory structural analysis of the wing may be performed without consideration of dynamic effects.

To investigate the effect of aspect ratio on the weight of the wing structure, the geometry of the FE-model was varied as shown in figure 5.1. It is worth noting that while most of the nodal

coordinates change with aspect ratio, the span of the centre-section remains constant in order to maintain a realistic connection to the fuselage. This is done by introducing a second design drawing to the system, similar to that in figure 2.1, but representing a version of the wing with a greater aspect ratio. Linear interpolation between the data in the two drawings results in the stretched meshes shown in fig. 5.1.

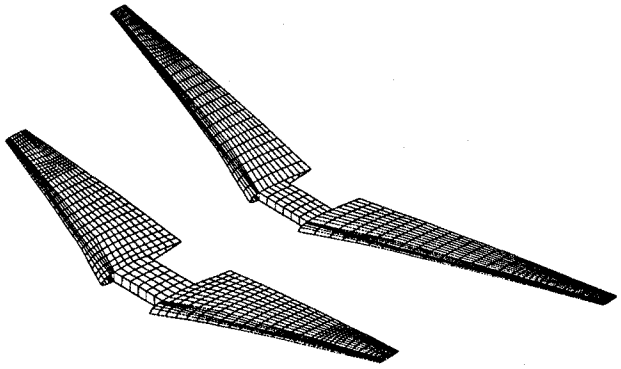

Figure 5.1: Variation of mesh geometry

The materials selected for the structure are Al 2024-T3 for the lower skin and Al 7075-T6 for all other components. Hat-section stringers are used in the upper skin, while Z-section stringers are used in the lower skin. The shear webs, including that of the auxiliary spar, are assumed to have double sided angle-section stiffeners throughout. The root rib is treated as a plate rib with Z-section stiffeners, and all other ribs are regarded as the standard truss type.

Only symmetric flight loading conditions have been considered. Maneuver and gust loads were derived according to FAR 25 regulations for a weight distribution corresponding to Maximum Zero Fuel Weight, and a flight altitude of 6100 m. Of these conditions, the most severe positive and negative loadings were selected as the structural design criteria. An additional set of three loading conditions, representing the 1-g cruise condition, the response to a 10 fps reference gust and the 1-g condition on the ground, are added for the purpose of generating fatigue loading spectrums for each stringer-skin panel.

For each loading condition, the pressure distribution on the wing was calculated using the panel method referred to in section 2.2. Since the definition of loading conditions in the classic flight envelope are based on the normal load factor, while the required input for the panel method consists of aircraft geometry, angle of attack and Mach number, the angles of attack that yield the required lift coefficients are found by interpolation between two trial values.

A suitable mass distribution, necessary to obtain a realistic inertia relief in the wing, was obtained by spreading out evenly the mass of the secondary structure (the fixed leading edge, high lift devices and aileron) over the elements in either the leading or trailing edge of the FE model. The weight prediction method used [1] also includes an estimation of the weight penalty due to the presence of joints, cut-outs and (landing gear) mountings. It should be noted that this secondary structure weight and the weight penalty for cut-outs etc. represent each approximately one quarter of the total wing weight. Hence the primary structure represented by the FE-model, contributes about one half of the total wing weight.

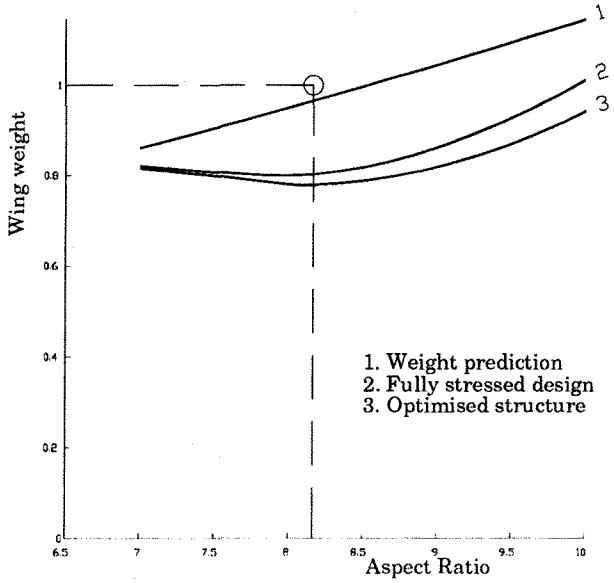

Figure 5.2: Wing weight as a function of aspect ratio

The element masses are discretised to form mass points, which with the appropriate accelerations, give the proper nodal inertia forces on the model. With the element properties and the loads defined, an initial FE analysis is performed, providing a first estimate of the loading intensity in the structure, the crushing loads on the ribs and the fatigue stress levels (the allowable fatigue stresses as derived in section 3.1 were in fact reduced considerably to match the F100 design practice). On the basis of this information, a first sub-level optimization is executed. As explained previously, the sub-level optimization increases or decreases the equivalent thicknesses to create a fully stressed design for each panel (no stiffness constraint was applied in this particular study). The total weight

of the structure created in this way is plotted in fig. 5.2 as the fully stressed design curve. It has been found that when a second FE analysis is performed based on these new equivalent thicknesses, little change occurs in the loading intensities in the skin panels, especially when there is no torsional stiffness constraint. This implies that the wing behaves much like a statically determinate structure, and that the fully stressed design procedure can be expected to yield a solution close to the optimal structure.

The optimal structure is generated using the allowable stresses found for the fully stressed design in an optimization of the model with thicknesses as previously determined in a main level optimization. The weight of this optimum structure is also plotted in figure 5.2. The weights in this figure have been made dimensionless by dividing by the actual Fokker 100 wing weight; hence a weight ratio of 1.0 implies exactly the correct F100 wing weight.

6. Conclusion

Due to the rapid generation of the FE-model, the effect of changes in aspect ratio are easily investigated. The FE-model serves as a basis for both a fully-stressed design and a formal optimization. In both cases a sub-level optimization of a simplified representation of the detail design is performed to determine realistic allowable stresses.

As seen in fig. 5.2, while the formal optimization produces a lower wing weight than the fully-stressed design, the differences are small, at least at the lower aspect ratios. In fact this is to be expected when the design is based entirely on strength requirements. The semi-empirical weight prediction is in good agreement with the actual wing weight. Not too much emphasis should be given to the difference between line 1 and lines 2-3 in fig. 5.2 at this stage of development of the program, because of uncertainties in the weight of the secondary structure, joints, etc., also because of the absence of stiffness constraints in both finite element procedures.

The results obtained, and the ease with which the modelling can be performed, encourage the view that the approach adopted can be successful in allowing an initial structural design to take place concurrently with other aspects at the preliminary design stage.

Acknowledgement

The authors wish to express their thanks to Fokker Aircraft BV for making available data for the Fokker 100, and to Ir. J. H. van der Sloot of that company for his participation in the project.

References

[1] Torenbeek, E.: *Development and Application of a Comprehensive, Design-Sensitive Weight Prediction Method for Wing Structures of Transport Category Aircraft*, Report LR-693, Delft University of Technology, Faculty of Aerospace Engineering, September 1992

[2] Bil, C., Dalen, F. van, Rothwell, A., Arendsen, P., Wiggenraad, J.F.M.: *Structural Optimization in Preliminary Aircraft Design: a Finite Element Approach*, ICAS-paper 92-6.7 R, 18th Congress of the International Council of the Aeronautical Sciences, September 20-25, Beijing 1992

[3] Bil, C.: *Development and Application of a Computer-Based System for Conceptual Aircraft Design*, ISBM 90-6275-484-8, Delft University Press, Delft 1988

[4] Bil, C.: *Aircraft Design and Analysis System (ADAS) Users Manual*, Handleiding LR-110, Delft University of Technology, Faculty of Aerospace Engineering, November 1992

[5] Kolk, J. Th. v.d., Sytsma, N. A., Sloof, J.W.: *Program PANEL, Version 1.0, Users Guide.* Memorandum AT-83-003 U, National Aerospace Laboratory, Amsterdam 1983

[6] Heyma, P.M.: *ADAS Implementation of a Panel Method for the Prediction of Aerodynamic Loads*, Report LR-723, Delft University of Technology, Faculty of Aerospace Engineering, June 1993

[7] Farrar, D. J.: *The Design of Compression Structures for Minimum Weight,* Journal of the Royal Aeronautical Society, November 1949

[8] An.: *Average Gust Frequencies Subsonic Transport Aircraft*, ESDU Data Item 69023, Fatigue-Endurance Data Section 1.3, March1989

[9] An.: *Frequencies of Vertical and Lateral Load Factors Resulting from Ground Manoeuvres of Aircraft*, ESDU Data Item 75008, Fatigue-Endurance Data Section 1.3, June 1982

[10] An.: *Flat Panels in Shear. Buckling of Long Panels with Transverse Stiffeners*, ESDU Data Item 02.03.02, Structures Sub-Series Vol. 10, April 1983

[11] An.: *Flat Panel in Shear. Post-Buckling Analysis*, ESDU Data Item 77014, Structures Sub-Series Vol. 10, April 1983

[12] Arendsen P.: *The B2000 Optimization Module: B2OPT*, NLR-Report TP 94116 L, National Aerospace Laboratory, Amsterdam, April 1994

[13] Merazzi, S.: *B2000 - A Modular Finite Element Analysis System. Version 1.0*, Memorandum SC-85-041 U, National Aerospace Laboratory, Amsterdam, June 1985

[14] An.: *MEM-COM, An Integrated Memory and Data Management System Version 6.0*, SMR Corporation, Bienne, Switserland, 1991

[15] Arendsen, P.: *PANOPT Theoretical Manual*, NLR-Report CR 93354 L, National Aerospace Laboratory, Amsterdam, August 1993

[16] Hooke,R., Jeeves, T.A.: *'Direct Search' Solution of Numerical and Statistical Problems*, Journal of the Association for Computing Machinery 8, 1961